

ORIGINAL ARTICLE



ASSESSMENT OF SOIL LOSS RISK USING INTEGRATED REMOTE SENSING AND GEOGRAPHIC INFORMATION SYSTEM (GIS) TECHNIQUES IN THE ARGANA BASIN, MOROCCO

| Said Ettazarini ^{1,2} | Mustapha El Jakani ^{1,2} | and | Khalid Najoui ^{1,2} |

¹. Centre Régional des Métiers de l'Education et de la Formation CRMEF Casablanca-Settat | Section SVT | Casablanca | Stendhal Av. PC 20340 | Casablanca | Morocco |

². Sidi Mohamed Ben Abdellah University| Natural Resources and Environment laboratory |Polydisciplinary Faculty of Taza | Taza | Morocco |

|Received | 27 March 2017| |Accepted | 30 April 2017| |Published 07 May 2017 |

ABSTRACT

Background: Soil loss by erosion processes remains the principal environmental issue in the Argana basin, in the western part of the Moroccan High Atlas. The erosion is a real threat not only for the durability of soil fertility, but also for the sustainability of Abdelmoumene dam due to its situation downstream. **Objectives:** This study is an attempt to assess the soil loss risk in the Argana basin by combining remote sensing and geographic information system (GIS) techniques as well as field observation. **Material and Methods:** The model used in this study was the Revised Universal Soil Loss Equation. Shuttle Radar Topography Mission (SRTM1) images with 30m of spatial resolution and Advanced Spaceborne Thermal Emission and Reflection (ASTER) Radiometer images, besides data obtained from the WorldClim 1.4 website and the Harmonized World Soil Database 1.2 (HWSD) were integrated and processed into an ArcGis environment to generate the soil loss risk map for the area studied. **Results:** The results mainly consist in thematic maps illustrating the distribution of the six factors considered in the revised universal soil loss equation RUSLE model, notably R, K, LS, C and P factors. Field observation confirmed that soils undergo deep erosion in zones of high to very severe erosion risk. **Conclusions:** It is concluded that the application of RUSLE model was helpful to assess the soil loss risk in the Argana basin. The annual mean of soil loss ranges from 0.036 to 270.572 (t/ha/year). Lands representing 17.23% of global surface showed low to moderate risk, while high to very high risk and severe to very severe risk were revealed in surfaces corresponding to 55.78% and 26.99% respectively. This situation is verified on field and reveals a real threat for both soils stability and Abdelmoumene dam durability. Anti-erosion measures are thus demanded to ensure sustainable protection of natural resources really threatened.

Keywords: Soil Erosion, RUSLE model, Risk mapping, Argana basin, Abdelmoumene dam, Morocco.

1. INTRODUCTION

Soil loss is a global and serious problem with negative environmental, economic and social impacts all over the world, especially in arid and semi-arid areas. In the Argana basin situated in the Moroccan High Atlas (fig. 1), soils are seen as a natural resource threatened by erosion. The loss of superficial soil leads to the reduction of its fertility necessary for sustainable agricultural development. In addition, the products of water erosion are transported downstream and can be accumulated in the reservoir of the Abdelmoumene dam, threatening thus its sustainability. A study of the soil erosion risk is therefore important to understand the erosive dynamics in the Argana basin and to plan anti-erosion measures for the priority zones . The Universal Soil Loss Equation USLE proposed by Wischmeier and Smith (1978) is the most used to estimate water erosion [1]. To adapt the USLE model and overcome the lack of data necessary for its use, modifications and approximations were made by other researchers leading thus to the Revised Universal Soil Loss Equation RUSLE [2,3,4,5,6,7]. Studies of the soil loss risk have been carried out in different parts of Morocco and under different natural conditions [8,9,10,11,12,13,14,15,16,17,18,19,20]. These and other works have shown the suitability of the USLE/RUSLE models to assess soil loss risk. The current level of knowledge and the available techniques relating to remote sensing and Geographic Information System (GIS) allow the choice of the most adapted formulas according to the data availability and to the natural conditions of the study area. In this work satellite images and universal databases as well as field data were processed in a GIS environment to develop a soil erosion risk map based on the RUSLE model.

2. MATERIALS AND METHODS

2.1 Study site:

The study area is about 1305 km² and is located in the western part of High Atlas, 70 km NE of the Agadir city (fig. 1). It stretches between north latitudes 30.640 to 31.073 and west longitudes -8.727 to -9.320 (decimal degrees, Mercich coordinate system, Morocco). Dominant outcrops are Permian-Triassic red deposits composed of conglomerates,

sandstones, silts and sandy clays with basalts and dolerites [21,22,23,24]. The Permian-Triassic formations are discordant on the Paleozoic basement, east of the area studied. The western part of the basin is characterized by outcrops of Jurassic age corresponding to limestone, clay limestone, sandstone, marl and sandy clay with gypsum [21,22].

Under arid to semi-arid climate conditions, human activities are mainly breeding, agriculture and arboriculture. The Abdelmoumene dam is built on the Issen River and being functional since 1981. It has a capacity up to 214 Mm³ and forms a water resource available to meet the needs of the population of the Souss area, between the foothills of the High Atlas mountains and the Souss River [25,26]. But due to environmental changes and soil degradation, erosion products are transported to the dam reservoir causing thus a possible decrease of its storage capacity and disturbance in the planning of sustainable development programs in the region.

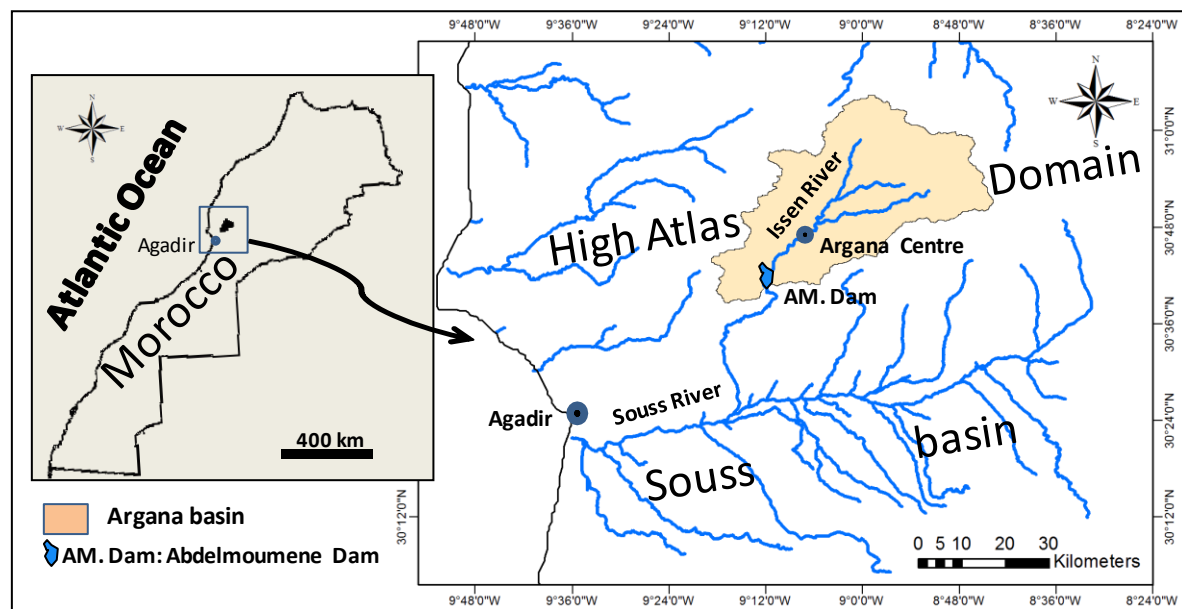


Figure 1: Location of the Argana basin in the Moroccan High Atlas domain

2.2 Data acquisition and processing:

Shuttle Radar Topography Mission satellite images SRTM1 with 30m of spatial resolution, acquired in September 2014 and downloaded from the USGS website at: <https://earthexplorer.usgs.gov>, were used to extract topographic and hydrographic data (e.g. slope, stream network, sub-basins and flow accumulation maps) necessary for the assessment of soil loss. Advanced Spaceborne Thermal Emission and Reflection ASTER Radiometer images, covering the study area and acquired between September and October 2014, were downloaded from the website of METI AIST Data Archive System MADAS at: <https://gbank.gsj.jp/madas/map/index.html> and used to assess the vegetation cover density and its contribution to soil conservation. Due to incomplete data on rainfall and soils in the region, monthly rainfall derived from long-term observations were provided by the WorldClim 1.4 universal free database based on interpolations of observed data representative of 1960-1990 and retrievable at: [27]. While soil data were obtained from the Harmonized World Soil Database HWSD 1.2 [28]. Besides information provided by the geological map of Argana [21] and aerial images, direct field observations were helpful to provide additional information and generate the soil loss risk map for the Argana basin. The approach adopted for processing the available data according to the RUSLE model consists in the integration of remote sensing and GIS techniques to assess soil loss risk. ArcGis software was very helpful to complete this task. Estimation of the soil loss potential is performed by using the RUSLE model. The revised equation uses the same principles as USLE but includes many improvements related to factor approximation and surface influence [29]. The factors used are erosivity of rainfall and runoff (R), soil erodibility (K), slope length impact (L), slope roughness (S), coverage and management practices (C) and conservation practices (P) [1]. The equation Eq.(1) is written as follows:

$$A = R \times K \times LS \times P \times C(1)$$

Where A is the annual mean of soil loss in (t/ha/year). R is expressed in (MJ.mm.ha⁻¹.h⁻¹.year⁻¹) and K in (t.h.MJ⁻¹.mm⁻¹) while L , S , C and P factors are dimensionless.

Rainfall-Runoff erosivity (R-factor)

The R-factor is a climatic parameter that takes into account the rainfall-runoff erosive capacity. It is determined by Wischmeier and Smith (1978, 1958) as the total of storm kinetic energy (E) multiplied by its maximum 30 min intensity (I_{30}) according to the following equation Eq.(2) [1-30]:

$$I = E \times I_{30} \quad (2)$$

The approximation adopted to estimate R-factor is based on monthly and annual rainfall data as suggested by Arnoldus (1980) [2]. It consists of a simple equation which is widely utilized and whose data are easy to obtain [16-31]. The equation is as follows Eq.(3):

$$R = \sum_{i=1}^{12} 1.735 \times 10^{\left(1.5 \times \log_{10} \frac{P_i^2}{P}\right) - 0.08188} \quad (3)$$

Where P_i represents the mean of monthly rainfall and P the mean of annual rainfall calculated as the sum of P_i . The R-factor is basically in U.S. unit (100ft.tonf.in/acre.h.year) and is multiplied by 17.2 for conversion into the international unit (MJ.mm.ha⁻¹.h⁻¹.year⁻¹) [3].

The R-factor map is derived from the processing of monthly mean rainfall data provided by Worlclim1.4 database. The subset covering the region of interest is extracted into ArcGis environment and annual mean rainfall as well as R-factor are generated as raster datasets.

Soil erodibility (K-factor)

Soil erodibility expresses the intrinsic capacity of a soil to be eroded by the effect of long-term rainfall-runoff. The K-factor depends on the soil parameters which are texture (M), organic matter (a), structure (S) and permeability (P). The equation used to evaluate soil erodibility is recommended for soils containing less than 70% silt [1-15-32,33]. This is the case of the Argana basin. The K-factor is expressed as follows Eq.(4):

$$K = \frac{1}{100} \times (2.1M^{1.14} \times 10^{-4}(12 - a) + 3.25(S - 2) + 2.5(P - 3)) \text{ for silt} \leq 70\% \quad (4)$$

Where M is the product of the primary particle size fractions Eq.(5):

$$M = (\%silt) \times (100 - \%clay) \quad (5)$$

a is obtained by multiplying the total organic Carbone provided by the HWSD database by 1.728. The K-factor expressed in U.S. unit (t.acre.h/100acre.ft.tonf.in) is multiplied by 0.1317 for conversion into the international unit (t.h.MJ⁻¹.mm⁻¹) [3]. The soil data concerning the area studied are extracted from HWSD database and processed in ArcGis to derive the soil erodibility map. Dominant soil type is loam with organic matter content varying from 1.088% to 3.38%. In this study, the soils are considered of moderately coarse texture and moderate permeability. The value 3 is therefore attributed to S and P in Eq.(4).

Slope length impact (L-factor)

Wischmeier and Smith (1978) considered the L-factor as a function of slope length as shown in Eq.(6) [1]:

$$L = \left(\frac{\lambda}{22.13}\right)^m \quad (6)$$

Where λ is the slope length and m is the slope exponent that varies between 0.2 and 0.5 for slope values between 0 and 5% and then remains invariant for slopes greater than 5%. However, the revision provided by the algorithm of McCool et al. (1987) considers that slope exponent varies according to the ratio of the rill and inter-rill erosion (F) [4]. The expression is shown in Eq.(7) [32-34,35,36].

$$m = \frac{F}{1+F} \text{ and } F = \frac{\frac{\sin(\alpha \times 0.01745)}{0.0896}}{3 \times (\sin(\alpha \times 0.01745))^{0.8} + 0.56} \quad (7)$$

The calculation of the L-factor is done by the use of the formula proposed by Desmet and Govers (1996) and expressed as follows, Eq.(8) [5]:

$$L_{ij} = \frac{(A_{ij} + D^2)^{m+1} - (A_{ij})^{m+1}}{x^m \times D^{m+2} \times 22.13^m} \quad (8)$$

Where A in (m^2) represents the contributing area at the inlet of the grid cell with coordinates (ij), D is the grid cell size in (m), x corresponds to the outflow direction for the grid cell and m is the slope length exponent.

SRTM1 satellite images are used to extract elevation data for the Argana basin as principal inputs to derive slope and flow accumulation maps, necessary to assess RUSLE L and S factors. The "Raster calculator" available in ArcGis environment was helpful to derive L map based on flow accumulation, with six grids (180 m) as the upper bound on the slope length, and slope steepness [29-37]. The used expression is as follows Eq.(9):

$$\frac{Power(flowacc+900, m+1) - Power(flowacc, m+1)}{Power(30, m+2) \times Power(22.13, m)} \quad (9)$$

Slope angle impact (S-factor)

The equations Eq.(10) and Eq.(11) are used to calculate the S-factor as proposed by McCool et al. (1987) [4]. The revised S-factor takes in the account the conditions of slope less and upper than 5.5 degrees [36-38].

$$S = 10.8 \times \sin \alpha + 0.03 \text{ for } \tan(slope) < 0.09 \quad (10)$$

$$S = 16.8 \times \sin \alpha - 0.5 \text{ for } \tan(slope) \geq 0.09 \quad (11)$$

The assessment of S-factor is performed by the use of "Raster calculator" tool and the following expression Eq.(11):

$$Con(\tan(slope) \times 0.01745) < 0.09, (10.8 \times \sin(slope \times 0.01745) + 0.03), (16.8 \times \sin(slope \times 0.01745) - 0.5)) \quad (11)$$

The topographic factor related to the slope shape is the result of slope length-slope angle interaction and has an effect on the magnitude of erosion [39]. Therefore, the effect of the slope length L and slope angle S are presented together as shown in Eq.(12):

$$LS = L \times S \quad (12)$$

Cover and management practice impact (C-factor)

The C-factor measures the combined effect of all the interrelated cover and management variables [1]. It is basically related to the nature and the density of the vegetation cover. Therefore, the value 1 is attributed to bare lands without protection and 0 to completely covered soils. The mostly used indicator of vegetation density is the Normalized Difference Vegetation Index NDVI that can be derived from the satellite images processing [40]. Van Der Knijff et al. (1999) proposed a scaling approach to calculate the C-factor as expressed in Eq.(13) [41].

$$C = e^{-\alpha \left(\frac{NDVI}{\beta - NDVI} \right)}, \quad \alpha = 2, \beta = 1 \quad (13)$$

Where α and β are dimensionless parameters that determine the shape of the curve relating to NDVI and C-factor. In this study, the selected values ($\alpha = 2$ and $\beta = 1$) provided good results in previous works [6-16-37-41,42,43].

ASTER images are used to assess the C-factor. Digital numbers (DN) of ASTER bands are converted to radiance then to reflectance values according to the ASTER users handbook instructions [44]. Reflectance raster datasets from band2 and band3, corresponding to red and near infrared bands respectively for ASTER radiometer, are integrated to calculate the NDVI and C-factor values as shown in Eq.(13).

Support practice impact (P-factor)

The P-factor is defined as the ratio of soil loss with a specific support practice to the corresponding loss with up-and-down-slope culture [1]. Practically, the field data enabled the mapping of agricultural lands and others. The SRTM1-derived elevation dataset was used to derive the slope percent, then P-factor values were attributed to agricultural lands according to the slope gradient as shown in table 1. All other lands were assigned a P-factor value of 1.

Table 1: P-factor values suggested by Wischmeier and Smith (1978) [1].

Land-use type	Slope (%)	P-factor
Agricultural lands	Slope < 5	0.10
	5 - 10	0.12
	10 - 20	0.14
	20 - 30	0.19
	30 - 50	0.25
	Slope > 50	0.33
	All	1.00

3. RESULTS

The integrated remote sensing and GIS techniques were helpful to follow the spatial distribution of RUSLE factors that control the soil erosion. The principal findings of this research are presented in figures 2 and 3.

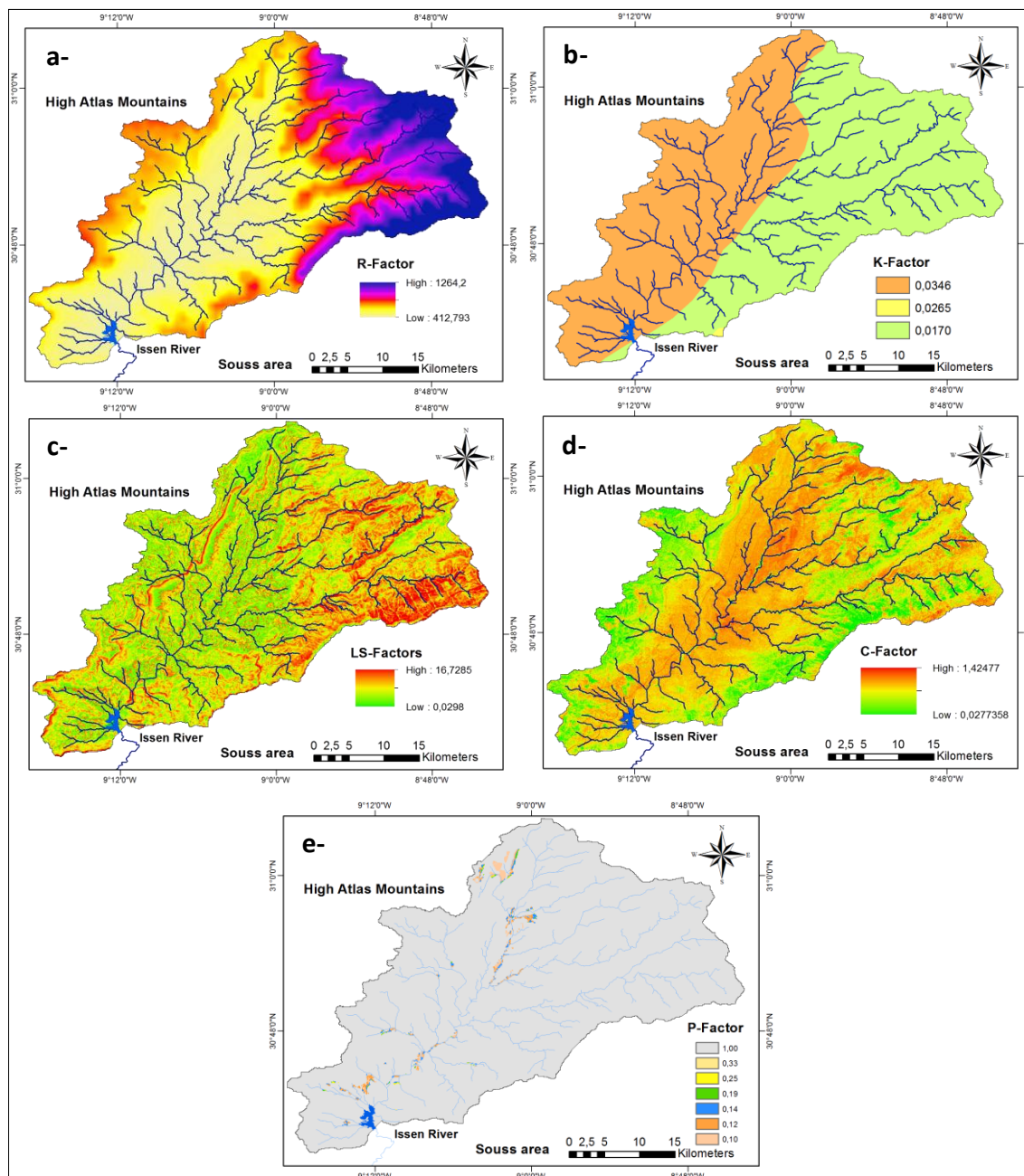


Figure 2: Spatial distribution of RUSLE factors assessed in the Argana basin. R-factor (a), K-factor (b), LS-factors (c), C-factor (d) and P-factor (e).

Rainfall-runoff impact (fig. 2a) shows values varying from 412 to 1264 ($\text{MJ.mm.ha}^{-1}.\text{h}^{-1}.\text{year}^{-1}$). Elevated lands, receiving mean annual rainfall up to 820mm, are highly exposed to rainfall-runoff erosion. They are situated in the eastern part of the basin. Soil erodibility is an important factor influencing the soil erosion. It corresponds to the K-factor that varies from

0.017 to 0.0346 ($t.h.MJ^{-1}.mm^{-1}$) in the Argana basin (fig. 2b). High values imply areas of high risk of erosion. This is the case of lands characterized by low contents of organic matter and clay particles. Figure 2c shows the spatial distribution of LS factors together, reflecting thus the impact of the slope shape. The values range from 0.03 to 16.73 and high values corresponding to high erosion risk are occurring in hilly areas. The C-factor assessment is based on the distribution of vegetation density. Figure 2d shows that C-factor values range from 0.0277 to 1.42 where high values imply the existence of degraded vegetation cover or bare soils exposed to the erosion. The support practice impact is insignificant in the Argana basin. Indeed the surface of agricultural lands represents only 1.42% of the area studied. The observed conservation measures mainly consist in contour plowing and terracing. The P-factor varies in these lands according to the slope steepness described in table 1 (fig. 2e). The main surface of the basin, close to 98.52% of the global area, has the P-factor value equal to 1.

The combination of the six RUSLE factors enabled the construction of the soil loss risk map (fig. 3) for the Argana basin. The area studied is subdivided into six severity categories according to the annual mean soil erosion rates as shown in table 2. Figure 3 shows that severe and very severe risk is mainly observed east of the basin, while low to moderate risk is mapped in the center of the area studied.

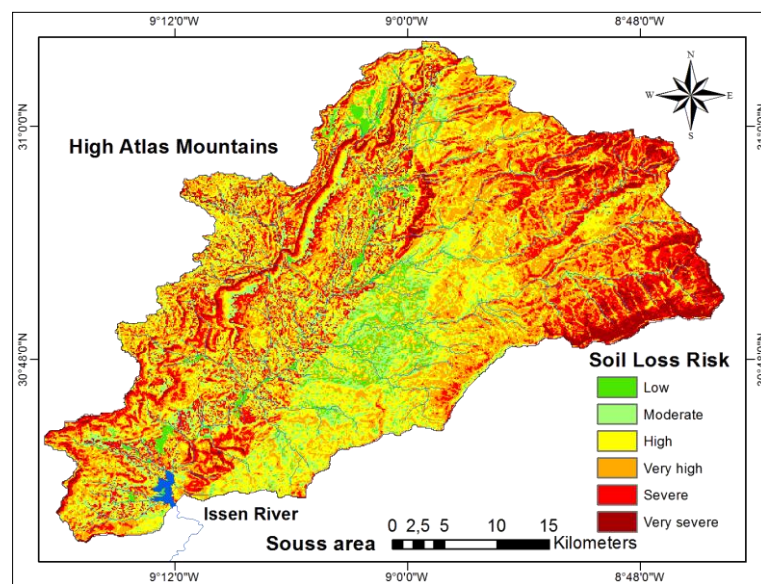


Figure 3: Distribution of the Soil Loss Risk assessed according the RUSLE model in the Argana basin.

Table 2: Annual soil erosion rates and severity distribution in the Argana basin.

Soil Loss (t/ha/year)	Severity classes	Area in (Km²)	Percent of global area
< 12	Low	51.58	03.95
12 - 25	Moderate	173.24	13.27
25 - 50	High	357.77	27.42
50 - 80	Very high	370.21	28.37
80 - 125	Severe	269.70	20.67
> 125	Very severe	82.50	06.32

The findings were verified by the field observation that confirmed the occurrence of deep erosion in zones of high to very severe risk of soil loss as it can be seen in figure 4. Figure 4a shows severe erosion affecting bare lands, while erosion in zones with degraded vegetation cover is revealed linked to steep slopes and stream network occurrence as shown in figure 4b. Deep erosion equally affects lands close to the Abdelmoumene dam and produces significant quantities of sediments that threaten the storage capacity of the dam (fig. 4c). Contrarily, reduced erosion is observed on gentle slopes at the center of the basin where the risk is revealed moderate to low (fig. 4d) and in zones protected by entropic practice such as terracing (fig. 4e) and contouring (fig. 4f).

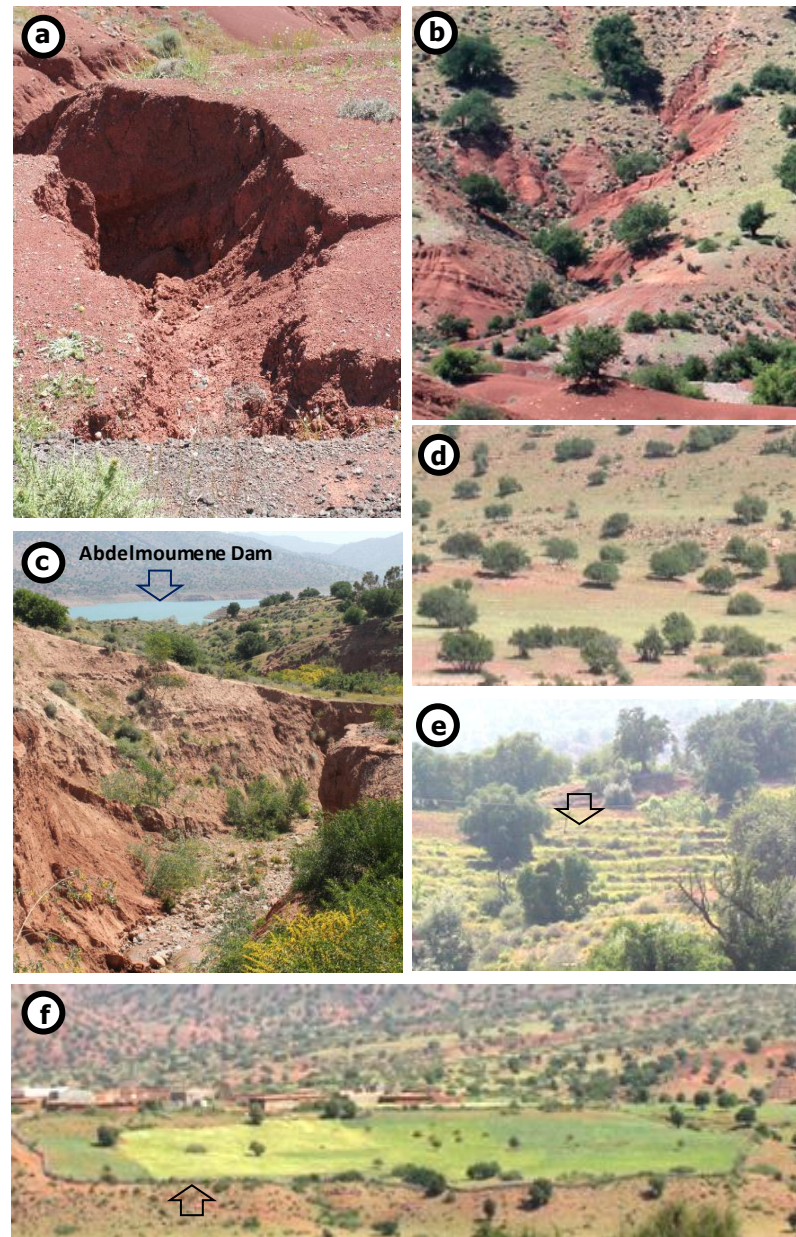


Figure 4: Field observation showing deep erosion affecting bare lands (a) and gully erosion on steep slopes with degraded vegetation cover (b), soil erosion by concentrated flow observed close to the water body of Abdelmoumene dam (c), reduced erosion in lands with moderate to low risk at the center of the basin (d) and protection practice including terracing (e) and contouring (f) as principal anti-erosion measures used in the area.

4. DISCUSSION

The soil loss risk depending on the interaction of natural and anthropologic factors, that vary in time and space, is assessed for the Argana basin by using the RUSLE model. The lands situated east of the Argana basin are of severe to very severe risk that is mainly controlled by the rainfall-runoff action. The soil erosion risk is linked to the steeper slopes occurrence in the western part of the area studied. While the soil texture as well as the organic matter amount are mainly controlling the soil erodibility and soil loss erosion at the center of the basin. The annual mean of soil loss ranges from 0.036 to 270.572 (t/ha/year). Lands of low to moderate risk represent 17.23% , while those of high to very high and severe to very severe risk constitute 55.78% and 26.99% respectively.

The findings relating to erosion in the Argana basin reveal an alarming situation, taking into account the large areas running a high to very severe risk of soil loss. The confirmation of threats by the erosion indicators through the field observation demonstrates that the risk is real. Indeed, the erosion of the soil leads to the mother-rocks exposure and thus to the soil poverty. In addition, the exposed roots of Argan trees imply severe erosion threatening this plant species, forming the focus of socio-economic activities in the region. The situation of the Abdelmoumene dam downstream of the

basin imposes drag measures to combat the filling of the reservoir. Anti-erosion measures in the Argana basin, upstream, remain the most cost-effective and sustainable approach.

5. CONCLUSION

The integration of remote sensing and GIS techniques provided the possibility to assess the soil erosion risk in the Argana basin, western High Atlas of Morocco. The use of satellite images, notably SRTM1 and ASTER, besides the exploitation of WorldClim and HWSD universal databases helped to overcome the limited availability of complete and pertinent data relating to rainfall and soil respectively. The RUSLE model was designed to develop the soil loss map and identify the areas of highest erosion risk and where conservation measures are demanded. This study showed that high to very severe erosion risk classes are revealed in 82.77% of lands in the Argana basin. The presented approach led to results in accordance with the field observations. Indeed, erosion indicators were observed in areas of high to very severe risk, while sedimentation was remarked in areas with an annual soil erosion value equal or close to 0. In this research it is demonstrated that the soil loss risk is real threatening thus soils as well as the Argan trees as principal natural resources necessary for the socio-economic development durability in the region. The soil erosion constitutes equally a real threat for the storage capacity of Abdelmoumene dam. Consequently, the investment in the improvement and multiplication of anti-erosive infrastructures is suggested as the most relevant and sustainable approach for conserving the different types of natural resources threatened.

6. REFERENCES

1. Wischmeier W.H., and Smith D.D. Predicting Rainfall Erosion Losses: A Guide to Conservation Planning. U.S. Department of Agriculture, Washington D.C., Agricultural Handbook no 537, Maryland; 1978.
2. Arnaldus H.M.J. An Approximation of the Rainfall Factor in the Universal Soil Loss Equation. In: De Boodt, M. and Gabriels D., Eds., *Assessment of Erosion*, John Wiley and Sons, New York, 1980, 127-132.
3. Foster G., McCool D., Renard K., and Moldenhauer W. Conversion of the universal soil loss equation to SI metric units. *Journal of Soil and Water Conservation*. 1981; (36):355-359.
4. McCool D.K., Brown L.C., and Foster G.R. Revised Slope Steepness Factor for the Universal Soil Loss Equation. *Transactions of the American Society of Agricultural Engineers*. 1987; (30):1387-1396. Available: <http://dx.doi.org/10.13031/2013.30576>
5. Desnet P.J.J., and Govers G. A GIS procedure for automatically calculating the USLE LS factor on topographically complex landscape units. *Journal of Soil and Water Conservation*. 1996; 51(5): 427-433.
6. Van der Knijff J.M., Jones R.J.A., and Montanarella L. Soil Erosion Risk Assessment in Europe. EUR 19044 EN, Office for Official Publications of the European Communities, Luxembourg, 34; 2000.
7. Renard K.G., Foster G.R., Weesies G.A., and Porter J.P. RUSLE: Revised universal soil loss equation. *Journal of Soil and Water Conservation*. 1991; 46(1):30-33.
8. Klik A., Kaitna R., and Badraoui M. Desertification Hazard in a Mountainous Ecosystem in the High Atlas Region, Morocco. 12th ISCO Conference on Sustainable utilization of global soil and water resources, May 26-31, Tsinghua University Press, Beijing, 2002, 636-644.
9. El Garouani A., Merzouk A., Jabrane R., and Boussema M.R. Cartographie de l'érosion des sols dans le bassin versant de l'Oued Jemaa (Pré-Rif, Maroc). *Géomaghabre*. 2003, (1):39-46.
10. El Garouani A., Chen H., Lewis L., Tribak A., and Abharour M. Cartographie de l'utilisation du sol et de l'érosion nette à partir des images satellitaires et du SIG IDRISI au Nord-Est du Maroc. *Télédétection, Editions Scientifiques GB*. 2008, 8 (3):193-201. Available: <https://hal.archives-ouvertes.fr/hal-00434258>
11. Bachaoui B., Bachaoui E., El Harti A., Bannari A., and El Ghmari A. Cartographie des zones à risque d'érosion hydrique: Exemple du Haut Atlas marocain. *Revue Télédétection*. 2007; 7(1-2-3-4):393-404. Available: <http://www.teledetection.net>
12. El Aroussi O., Mesrar L., Lakrim M., El Garouani A., and Jabrane R. Methodological approach for assessing the potential risk of soil erosion using remote sensing and GIS in the Oued El Malleh watershed (Pre-Rif, Morocco). *Journal of Materials and Environmental Science*. 2011; 2(1):433-438. Available: http://www.jmaterenvironsci.com/Document/vol2/vol2_S1/2-EL%20AROUSSI%20theme1.pdf
13. Mahdioui L., Chaïrhami H., Allali H., Naja J., and Bakkali A. Spatial modeling and assessment of soil loss of watershed Oued Bou Moussa, High Chaouia, Settat, Morocco. *International Journal of Latest Research in Science and Technology*. 2014; 3(4):18-21. Available: <http://www.mnkjournals.com/jilrst.htm>
14. Tahiri M., Tabyaoui H., El Hammichi F., Tahiri A., and El Hadi H. Evaluation et Quantification de l'Erosion et la Sédimentation à Partir des Modèles RUSLE, MUSLE et Déposition Intégrés dans un SIG. Application au Sous-Bassin de l'Oued Sania (Bassin de Tahaddart, Rif nord occidental, Maroc). *European Journal of Scientific Research*. 2014; 125(2):157-178. Available: <http://www.europeanjournalofscientificresearch.com>
15. Lahlaoui H., Rhinane H., Hilali A., Lahssini S., and Khalil L. Potential Erosion Risk Calculation Using Remote Sensing and GIS in Oued El Maleh Watershed, Morocco. *Journal of Geographic Information System*. 2015; 7:128-139. Available: <http://dx.doi.org/10.4236/jgis.2015.72012>
16. Belasri A., and Lakhoui A. Estimation of Soil Erosion Risk Using the Universal Soil Loss Equation (USLE) and Geo-Information Technology in Oued El Makhazine Watershed, Morocco. *Journal of Geographic Information System*. 2016; 8:98-107. Available: <http://dx.doi.org/10.4236/jgis.2016.81010>
17. Chadli K. Estimation of soil loss using RUSLE model for Sebou watershed (Morocco). *Modeling Earth Systems and Environment*. 2016; 2:51. Available: <http://dx.doi.org/10.1007/s40808-016-0105-y>
18. Khali Issa L., Lech-Hab K.B.H., Raisouni A., and El Arrim A. Quantitative Mapping of Soil Erosion Risk Using GIS/USLE Approach at the Kalaya Watershed (North Western Morocco). *Journal of Materials and Environmental Science*. 2016; 7(8):2778-2795. Available: http://www.jmaterenvironsci.com/Document/vol7/vol7_N8/291-JMES-2151-Khali%20Issa.pdf
19. Iaaich H., Moussadek R., Baghdad B., Mrabet R., Douaik A., Derradji A., and Bouabdli A. Soil erodibility mapping using three approaches in the Tangiers province, Northern Morocco. *International Soil and Water Conservation Research*. 2016; 4:159-167. Available: <http://dx.doi.org/10.1016/j.iswcr.2016.07.001>
20. Melihou M., Khattabi A., Mhammdi N., and Hongming Z. Impact of Land Use and Vegetation Cover on Risks of Erosion in the Ourika Watershed (Morocco). *American Journal of Engineering Research*. 2016; 5(9):75-82. Available: [http://www.ajer.org/papers/v5\(09\)/L0509075082.pdf](http://www.ajer.org/papers/v5(09)/L0509075082.pdf)
21. Tixeront M. Lithostratigraphie et minéralisations cuprifères et uranifères stratiformes syngénétiques et familières des formations détritiques permo-triasiques du couloir d'Argana, Haut Atlas occidental, Maroc. *Notes et Mémoires du Service Géologique du Maroc*. 1973; 33(249):147-177
22. Tixeront M. Carte géologique et minéralisations du couloir d'Argana, Haut Atlas occidental, Maroc. *Notes et Mémoires du Service Géologique du Maroc*. 1974; n° 205.
23. Jalil N. Les vertébrés permiens et triasiques d'Afrique du Nord, avec une description de nouveaux Parareptiles Paracerasaures (Amniota, Parareptilia, Pareiasauria) du Permien du Maroc. Liste faunistique relations phylogénétiques et implications biostratigraphiques. Thesis, University of Cadi Ayyad, Marrakech, 2001, 209 p.
24. Medina F., Vachard D., Colin J.P., Ouarhache D., and Ahmamou M. Charophytes et ostracodes du niveau carbonaté de Taourirt Imzilien (Membre d'Aghjal, Trias d'Argana); implications stratigraphiques. *Bulletin de l'Institut Scientifique. Section Sciences de la Terre*. 2001; 23:21-26. Available: [http://www.israbat.ac.ma/wp-content/uploads/2015/03/03-%20Medina%20et%20al.%20\(21-26\).pdf](http://www.israbat.ac.ma/wp-content/uploads/2015/03/03-%20Medina%20et%20al.%20(21-26).pdf)

25. Choukr-Allah R., Bellouch H., and Baroud A. Gestion intégrée des ressources en eau dans les bassins du Souss Massa. In : Karam F. (ed.), Karra K. (ed.), Lamaddalena N. (ed.), Bogliotti C. (ed.). Harmonization and integration of water saving options. Convention and promotion of water saving policies and guidelines. Bari : CIHEAM / EUDG Research , p. 67-69 (Options Méditerranéennes : Série B. Etudes et Recherches; n. 59); 2007.

26. Boujnikh M., and Humbert A. Water in the Souss basin: competition and disorganization of the rural systems. *Norois*. 2010;214(1):113-126. Available: <https://norois.reviews.org/3178>

27. Hijmans R.J., Cameron S.E., Parra J.L., Jones P.G., and Jarvis A. Very high resolution interpolated climate surfaces for global land areas. *International Journal of Climatology*. 2005; 25:1965-1978. Available: <http://onlinelibrary.wiley.com/doi/10.1002/joc.1276/pdf>

28. FAO/IIASA/ISRIC/ISSCAS/JRC. Harmonized World Soil Database (version 1.2). FAO, Rome, Italy and IIASA, Luxemburg, Austria. 2012, Available: http://webarchive.iiasa.ac.at/Research/LUC/External-World-soil-database/HTML/HWSD_Data.html?sb=4

29. Jabbar M.T. Application of GIS to Estimate Soil Erosion Using USLE. *Geo-Spatial Information Science*. 2003; 6(1):34-37. Available: <http://dx.doi.org/10.1007/BF02826699>

30. Wischmeier W.H., Smith D.D., and Uhland R.E. Evaluation of factors in the soil-loss equation. *Agricultural Engineering*. 1958; 39:458-462.

31. Wang R., Zhang S., Yang J., Pu L., Yang C., Yu L., Chang L. and Bu K. Integrated Use of GCM, RS, and GIS for the Assessment of Hillslope and Gully Erosion in the Mushi River Sub-Catchment, Northeast China. *Sustainability*. 2016; 8, 317. Available: <http://dx.doi.org/10.3390/su8040317>

32. Renard K.G., Foster G.R., Weesies G.A., McCool D.K., and Yoder D.C. Predicting Soil Erosion by Water: A Guide to Conservation Planning with the Revised Universal Soil Loss Equation (RUSLE). Agriculture Handbook No.703, US Department of Agriculture, Washington DC, 1997, 1-251.

33. Elbouqdaoui K., Ezzine H., Badraoui M., Rouchdi M., Zahraoui M., and Ozer A. Evaluation by remote sensing and SIG of potential erosion risk in the Oued Srou Basin (Middle Atlas, Morocco). *Geo-Eco-Trop*. 2005; 29:25-36. Available: <http://www.geocetrop.be/index.php?page=numero-29>

34. McCool D.K., Foster G.R., Mutchler C.K., and Meyer L.D. Revised slope length factor for the universal soil loss equation. *Trans. ASAE*. 1989; 32(5):1571-1576. Available: <http://dx.doi.org/10.13031/2013.31192>

35. Liu B.Y., Nearing M.A., Shi P.J., and Jia Z.W. Slope Length Effects on Soil Loss for Steep Slopes. *Soil Science Society of America Journal*. 2000; 64:1759-1763. Available: <http://dx.doi.org/10.2136/sssaj2000.6451759x>

36. Oliveira P.T.S., Rodrigues D.B.B., Sobrinho T.A., Panachuki E., and Wendland E. Use of SRTM data to calculate the (R)USLE topographic factor. *Maringá Technology. Acta Scientiarum*. 2013; 35(3):507-513. Available: <http://dx.doi.org/10.4025/actascitechnol.v35i3.15792>

37. Parveen R., and Kumar U. Integrated Approach of Universal Soil Loss Equation (USLE) and Geographical Information System (GIS) for Soil Loss Risk Assessment in Upper South Koel Basin, Jharkhand. *Journal of Geographic Information System*. 2012; 4:588-596 Available: <http://dx.doi.org/10.4236/jgis.2012.46061>

38. Oliveira J. A., Dominguez J. M. L., Nearing M. A., and Oliveira P. T. S. A GIS-based procedure for automatically calculating soil loss from the Universal Loss Equation: GISUS-M. *Applied Engineering in Agriculture*. 2015; 31(6):907-917. Available: <http://dx.doi.org/10.13031/aea.31.11093>

39. Edwards K. Runoff and Soil Loss Studies in New South Wales, Technical Handbook No. 10. Soil Conservation Service of NSW, Sydney, 1987.

40. Sader S.A., and Winne J.C. RGB-NDVI Colour Composites for Visualizing Forest Change Dynamics. *International Journal of Remote Sensing*,. 1992; 13(16):3055-3067. Available: <http://dx.doi.org/10.1080/01431169208904102>

41. Van Der Knijff J.M., Jones R.J.A., and Montanarella L. Soil erosion risk assessment in Italy. Ispra: European Commission Directorate General JRC, Joint Research Centre Space Applications Institute. European Soil Bureau; 1999.

42. Van Leeuwen W.J.D., and Sammons G. Vegetation Dynamics and Soil Erosion Modeling Using Remotely Sensed Data (MODIS) and GIS. Proceedings of the Tenth Biennial USDA Forest Service Remote Sensing Applications Conference On Remote Sensing for Field Users, April 5-9, Salt Lake City, 2004

43. Kouli M., Soupios P., and Vallianatos F. Soil erosion prediction using the Revised Universal Soil Loss Equation (RUSLE) in a GIS framework, Chania, Northwestern Crete, Greece. *Environmental Geology*. 2009;57(3):483-497. Available: <http://dx.doi.org/10.1007/s00254-008-1318-9>

44. Abrams M., and Hook S. ASTER User Handbook (version 2). Jet Propulsion Laboratory, Pasadena, CA-91109, USA. 135 pp; 2001.

Cite this article: Said Ettazarini, Mustapha El Jakani, and Khalid Najoui. ASSESSMENT OF SOIL LOSS RISK USING INTEGRATED REMOTE SENSING AND GEOGRAPHIC INFORMATION SYSTEM (GIS) TECHNIQUES IN THE ARGANA BASIN, MOROCCO. *Am. J. innov. res. appl. sci.* 2017; 4(5): 186-194.

This is an Open Access article distributed in accordance with the Creative Commons Attribution Non Commercial (CC BY-NC 4.0) license, which permits others to distribute, remix, adapt, build upon this work non-commercially, and license their derivative works on different terms, provided the original work is properly cited and the use is non-commercial. See: <http://creativecommons.org/licenses/by-nc/4.0/>